Laser and Particle Beams (2004), *22*, 157–162. Printed in the USA.

DOI: 10.1017/S0263034604222108

On the inefficiency of hole boring in fast ignition

P. MULSER AND R. SCHNEIDER
Theoretical Quantum Electronics (TQE), Darmstadt University of Technology, Darmstadt, Germany
(RECEIVED 27 June 2003; ACCEPTED 31 August 2003)

Abstract

Hole boring and fast ignition seem to exclude each other: When there is hole boring, no ignition occurs, and vice versa. The laser beam pressure only causes a more or less deep cone-shaped critical surface that leads to better guidance of the beam and to improved laser–plasma coupling. At laser wavelengths of the order of 1 μm, successful fast ignition requires strong anomalous laser beam–pellet coupling.

Keywords: Fast ignition; High burn efficiency; Hole boring; Laser beam pressure

1. INTRODUCTION

For inertial confinement fusion (ICF) to work successfully a sufficient amount of precompressed DT fuel must be brought up to a temperature of 6–10 keV to induce a self-sustaining nuclear burn wave. This is either accomplished by central spark ignition, where the fast heating is provided by a converging spherical shock wave, or by fast ignition (FI), with a superintense laser beam during a time interval of 10–30 ps. The extension R of the hot spot is determined by the density ρ of the compressed fuel through $\rho R \geq 0.3$ gcm^{-2} (Lindl, 1995).

The concept of FI is attractive because it offers several advantages: (1) high burn efficiency (25%), (2) no special symmetry constraints, and (3) reduced growth of hydrodynamic instabilities. However, they contrast with the fact that the laser can deposit its energy at densities not exceeding the critical density ρ_c, respectively particle density n_c. As a consequence, electrons of relativistic energies must provide for the energy transport to the dense compressed fuel in an efficient way, that is, good collimation, and on a time scale of several tens of picoseconds (e.g., 70 ps; Hain & Mulser, 2001). Essentially three scenarios have been proposed to achieve the goal: (1) fast beam ignition (FBI) by converting the relativistic electron beam into a focused beam of ions that is absorbed in a controlled way in the compressed pellet core; (2) cone-guided fast ignition (CFI), where a hollow high-Z cone (e.g., gold) is placed in the fusion pellet with its top reaching the core to bring the absorbing critical region very close to the ignition region (Kodama *et al.*, 2001); (3) fast coronal ignition (FCI), with the critical density brought as close as possible to the compressed core by hole boring. This appealing scheme came up nearly 10 years ago and has meanwhile apparently been accepted as a realizable FI scenario. It is therefore surprising that a detailed study of FCI combined with hole boring has not been undertaken so far. The advantages of the scheme are evident. If, for instance, a laser beam can drill a hole in the pre-compressed pellet up to the density $\rho \simeq 200$ gcm^{-3} the energy spread of the hot electron beam could be significantly reduced and perhaps better coupling of the FI laser beam, now being guided by the walls of the hole, would be an additional advantage. By deep hole boring, the use of a cone could be avoided and CFI would reduce to FCI. In this article we show that, unfortunately, hole boring in connection with FI cannot work properly: FI and hole boring nearly exclude each other.

Address correspondence and reprint requests to: P. Mulser, Theoretical Quantum electronics (TQE), Darmstadt University of Technology, Schlossgartenstr. 7, D-64289 Darmstadt, Germany. E-mail: peter.mulser@physik.tu-darmstadt.de

2. HOLEBORING IN COLD MATTER

Imagine impinging a laser beam of intensity $I = \epsilon_0 c\hat{E}^2/2$ onto the critical density of a pre-compressed pellet of local pressure p_0. The laser beam acts like a piston under pressure P_A, which is the sum of the light pressure $p_L = (1 + R)I/c$, where R is the reflection coefficient and c is the light speed, and the ablation pressure $p_A = p_c + \rho_c v_c^2 = p_c(1 + M_c^2)$; hence, with $\mu = I/2cp_c$,

$$P_A = (1+R)\frac{I}{c} + p_c(1+M_c^2) \tag{1}$$

$$M_c = \begin{cases} \dfrac{\mu}{\exp(\mu+0.5)-2} & \mu > 1 \\ 1-\sqrt{0.4\mu} & \mu \le 1 \end{cases}$$

(Mulser *et al.*, 2003). p_c and M_c are the plasma pressure and Mach number at the critical point. Equation (1) is obtained for a one-dimensional (1D) plasma flow and T_e = const in the evanescent region whose extension, owing to profile steepening, is less than a quarter laser wavelength. Under the action of P_A, a bow shock S traveling at speed v_0 forms (Fig. 1a). In the infinitesimal time dt, the amount of matter $\rho_0 v_0\, dt$ undergoes the velocity change from $v = 0$ to $v = v_1$, the density change from ρ_0 to ρ_1 and the pressure change from p_0 to p_1 when crossing S. With the compression ratio $\kappa = \rho_1/\rho_0$ holds along the symmetry axis $v_1 = v_0(1-\kappa^{-1})$, and hence, the momentum balance reads

$$P_A = \rho_0 v_0^2(1-\kappa^{-1}) + p_0. \tag{2}$$

First $p_A = n_c kT_e(1+M_c^2)$ must be evaluated in relation to p_L. The intensity interval of relevance is $I = 10^{19}$–10^{21} W cm^{-2}. The wavelengths considered are λ = 800 nm (Ti:Sa) and λ = 248 nm (KrF). The effective (i.e., relativistic) critical density $n_c = \gamma_{\rm eff} n_{c0}$ is calculated from formulas given in the literature (Mulser & Bauer, 2003):

$$\gamma_{\rm eff} = \frac{\pi\gamma_{\rm th}}{\displaystyle\int_0^{2\pi} d\xi \cos^2\xi\{1+(\alpha/\gamma_{\rm th})^2\cos^2\xi\}^{-1/2}} \tag{3}$$

$$\alpha = e\hat{A}/m_e c, \quad \hat{A} = \hat{E}/\omega.$$

$\gamma_{\rm th}$ is defined by Eq. (4). For $\alpha/\gamma_{\rm th} = 1$ results $\gamma_{\rm eff} = (1+0.5)^{1/2}\gamma_{\rm th}$, for $\alpha/\gamma_{\rm th} \simeq 2$ follows $\gamma_{\rm eff} = (1+0.8(\alpha/\gamma_{\rm th})^2)^{1/2}\gamma_{\rm th}$; for $(\alpha/\gamma_{\rm th}) > 5$ $\gamma_{\rm eff}$ approaches the asymptotic value $\gamma_{\rm eff} = 0.785\alpha$. This behavior is of great help in preparing Table 1. The relativistic γ-factor used here is considerably different from simple standard expressions generally used.

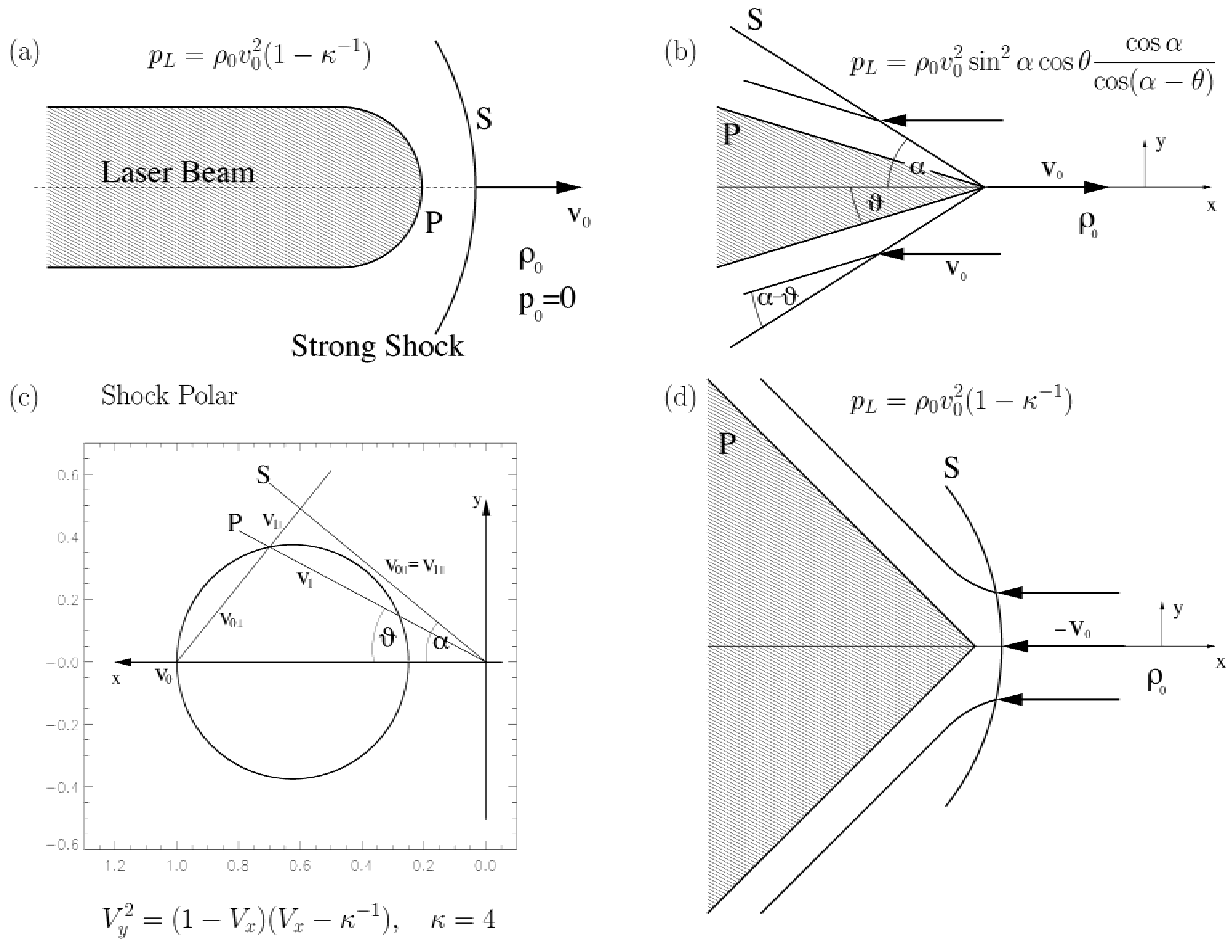

Fig. 1. Holeboring in cold matter: alternative models for matter displacement. a: Laser acts as impermeable piston; P_A: piston pressure, ρ_0: undisturbed pre-compressed pellet density, v_0: hole boring speed. Oblique shock (b) is determined from the shock polar (c). Beyond limiting angle θ shock detaches from cone (d).

https://doi.org/10.1017/S0263034604222108 Published online by Cambridge University Press

Table 1. *Ratio of ablation pressure p_A to light pressure p_L as a function of laser intensity I*

Laser	n_{c0} [cm^{-3}]	I [W cm^{-2}]	γ_{eff}	M_c	T_e [MeV]	p_A/p_L
Ti:Sa	1.8×10^{21}	1×10^{19}	2.2	0.44	0.39	0.72
		2×10^{20}	9.0	0.23	1.26	0.30
		2×10^{21}	20.0	0.21	5.29	0.28
KrF	1.8×10^{22}	1×10^{19}	1.2	0.46	0.12	0.84
		2×10^{20}	3.0	0.31	0.49	0.41
		2×10^{21}	8.8	0.23	1.29	0.30

A lower limit of the electron kinetic temperature T_e is obtained from the requirement that under steady-state conditions the absorbed photon flux $(1-R)I$ must equalize the electron energy flux q_e into the pellet. We set

$$(1-R)I = q_e = \begin{cases} \frac{1}{2}\, kT_e n_c \left(\frac{kT_e}{m_e}\right)^{1/2}, & \text{non-rel.} \\ kT_e n_c v_e = \left(\gamma_{\text{th}} - \frac{1}{\gamma_{\text{th}}}\right) n_c m_e c^3, & \text{rel.} \\ kT_e = (\gamma_{\text{th}}{}^2 - 1)^{1/2} m_e c^2 \end{cases} \quad (4)$$

Depending on the divergence of the electron beam q_e, there is an uncertainty factor of order unity in this definition of T_e. For comparison, if in the nonrelativistic expression for q_e an isotropic Maxwellian distribution is used, the correct numerical factor is $2(2/\pi)^{1/2} = 1.6$; instead for a collimated, that is, one-dimensional (1D), Maxwellian, it is $(2\pi)^{-1/2} = 0.4$. For the critical pressure we set $p_c = n_c kT_e$. In the nonrelativistic case the pressure in one dimension is twice the internal energy $\langle E\rangle$, in three dimensions (isotropic) it is two thirds of it, regardless of whether the electron distribution is a Maxwellian or any other distribution. The relativistic case is more complicated. Fortunately it becomes simple again for superrelativistic electrons, that is, $q_e = kT_e n_c c$ if $m_e c^2 \ll kT_e$. Furthermore, in one dimension, $p = n\langle E\rangle$ and in three dimensions, $p = \frac{1}{3} n\langle E\rangle$ holds (e.g., see the photon gas).

In Table 1 n_{c0}, γ_{eff}, M_c, T_e, and p_A/p_L are given for the intensities $I = 10^{19}$, 2×10^{20}, 2×10^{21} W cm^{-2} and for $R = 0.5$. An absorption of 50% is a realistic assumption (see, e.g., Feurer *et al.*, 1997; Ruhl *et al.*, 1999). The plasma pressure in the undisturbed pellet before the laser beam arrives is set equal to zero.

From Table 1 important information is extracted regarding the temperature T_e, its dependence on the laser wavelength, and the pressure ratio p_A/p_L. Numerical FI studies do not give much chance to successful ignition for energy flux densities q_e significantly less, for example, by a factor of 3, than $q_e = 10^{21}$ W cm^{-2} (Mulser & Bauer, 2003). At Ti:Sa wavelength and 10^{21} W cm^{-2} absorbed laser intensity, T_e amounts to 5.3 MeV, even though the relativistic increase of n_{c0} is the considerable factor of 20. Because no effect is known so far which would lead to overdense light beam penetration, this temperature is a very reliable lower limit. Unless there occurs very anomalous collective coupling of such energetic electrons to the cold background, the electron beam is not stopped by the pre-compressed pellet and FI fails at $\lambda \gtrsim 1$ μm wavelength.

Table 1 underlines the importance of transport and collective deposition research at relativistic intensities. Switching to KrF lasers is a remedy; however it brings T_e down only by a factor of 4 instead of the wavelength ratio squared, that is, 10.4, because with shorter wavelength the relativistic α-factor reduces also and hence γ_{eff} lowers from $\gamma_{\text{eff}} = 20$ to $\gamma_{\text{eff}} = 9$. One has to bear in mind that $T_e = 1.29$ MeV is a lower limit. Future experiments have to show whether absorption takes place at n_c, increasing according to Eq. (3), or whether, due to enormous profile steepening at the critical point, laser beam penetration follows a more modest density increase.

Another important aspect is that the hole boring bow shock always runs into a preheated region of pressure $p_0 \geq p_c$ because the electron energy transport is faster than v_0. Therefore the maximum effective pressure determining the hole boring speed v_0 is $P_A - p_0 = p_L + p_c(1 + M_c^2)$. For all intensities considered in Table 1 $P_A - p_c$ is very close to p_L.

The efficiency of hole boring in a cold background plasma (almost no energy exchange of the electrons from the critical region) may be studied by assuming a pellet density profile of the form $\rho_0 = h(x/L)^s$. From the pressure balance (2), $P_A = f\rho_0 v_0^2 + p_c$, $f = (1 - \kappa^{-1})$, the depth x/L as a function of t is given by

$$\frac{x}{L} = \left(\frac{s+2}{2L}\, t\right)^{2/(s+2)} \left(\frac{P_A - p_c}{fh}\right)^{1/(s+2)}. \quad (5)$$

The pressure balance (2) also holds in the absence of a shock, that is, $f = 0$. Choosing $I = 2\times10^{21}$, $R = 0.5$, $h = 400$ gcm^{-3}, $t = 20$ ps, $f = 0.5$ (corresponding to $\kappa = 2$, typical compression in numerical simulations), $L = 0.01$ cm and $s = 2$, one finds with $P_A - p_c = 1.5\times1.05 p_L$ (see Table 1) $x/L = 0.45$, $\rho/h = 0.21$, $\rho = 83$ gcm^{-3}. With the exponent $s = 3$, $x/L = 0.53$, $\rho/h = 0.15$, $\rho = 59$ gcm^{-3}. Now a typical "hole boring prepulse," frequently quoted in the literature, of $I = 10^{19}$ W cm^{-2}, $P_A - p_c = 1.5\times1.2$ (Table 1), $s = 2$, and $t = 50$ fs is considered: $x/L = 0.23$, $\rho/h = 0.055$, $\rho = 22$ gcm^{-3}. After 20 ps, the laser has penetrated up to $\rho = 8$ gcm^{-3} only. Thus, at such an intensity hole boring is rather modest even in the most favorable case of cold plasma.

There remain some uncertainties originating from the laser pulse transverse intensity distribution and beam width, in the bow-shock model all summarized by the factor f. It is therefore illuminating to use an alternative model that is also accessible to an analytical treatment. As soon as the bow shock invades a density region $\rho_0 \gtrsim 1$ gcm^{-3} (i.e., 5 times solid DT) the mass flows $p_c M_c$ and $\rho_0 v_0$ obey the inequality $p_c M_c \ll \rho_0 v_0$. As a consequence, there is nearly stagnation on the axis in front of the piston P. This means that the laser acts nearly like an impermeable piston, devi-

https://doi.org/10.1017/S0263034604222108 Published online by Cambridge University Press

ating almost all plasma laterally. Therefore a solid cone-shaped piston of narrow aperture angle θ propagating at speed v_0 is considered. From the vertex of the piston P a coaxial conical shock of aperture angle α originates (Fig. 1b). Under the assumption of negligible pressure p_0, the possible states behind the shock cone (region 1) can be determined from the shock polar, which in Fig. 1c is given for $\kappa = 4$. When normalized to v_0 it reads $V_y^2 = (1 - V_x)(V_x - \kappa^{-1})$. From the continuous transition of the tangential component through the shock front, that is, $v_{0\parallel} = v_{1\parallel}$ (see, e.g., any textbook of gas dynamics), one derives

$$P_A - p_0 = \rho_0 v_0 v_1 \sin^2\alpha \cos\theta = \rho_0 v_0^2 \sin^2\theta \frac{\cos\alpha}{\cos(\alpha - \vartheta)}. \quad (6)$$

For angles θ such that the straight line starting from the origin does not have any point in common with the shock polar, the shock S forms at a finite distance from the cone with finite curvature on the axis (Fig. 1c), and Eq. (2) applies again. For a strong shock, equivalent to $p_0 = 0$, the limiting angle is given by $\tan\theta = (\kappa - 1)/2\kappa^{1/2}$. For $\kappa = 4$ results, $\tan\theta = \frac{3}{4}$ and $\theta = 37°$. The corresponding angle α follows from Figure 1, that is, $\theta = 64°$, and the angular factor in Eq. (6), corresponding to the f-factor of Eq. (5), assumes the value 0.32. For the cone and shock angles of $\theta = 28°$ and $\alpha = 40°$ indicated in Figure 1, the angular factor is 0.29. The factor decreases monotonically with decreasing aperture angle of the cone and, at given $P_A - p_0$, v_0 increases. For a strong shock of Figure 1a,c the factor becomes $f = 1 - \frac{1}{4} = 0.75$. The comparison of the two models shows that a laser beam with a narrow cone-shaped intensity profile accelerates hole boring owing to an f-factor less than 0.5 in the denominator of Eq. (5): with $f = 0.29$, x/L increases by a factor of 1.15 ($s = 2$) and 1.11 ($s = 3$). The conclusion, also to the authors' surprise, is that even in the most favorable situation of cold matter, that is, collimated hot electrons interacting with the dense pellet core only, hole boring at all relevant laser beam intensities is not very efficient.

3. HOLEBORING IN HOT MATTER

3.1. Numerical results

First of all, there is the experience with computer simulations of FI on the absence of any hole boring. Specifically, a 5-mg DT pellet, pre-compressed to 350 gcm^{-3}, was successfully ignited by a 75 kJ laser beam of absorbed intensity of $I = 10^{21}$ W cm^{-2}, deposited at the density $\rho = 4.6$ gcm^{-3} during 20 ps (Mulser & Bauer, 2003). The energy transport was accomplished by flux-limited Spitzer-diffusive heat conduction, and $R = 0$, that is, no reflection, was set. During the entire time of irradiation no indication of hole boring or concave deposition surface deformation could be observed. It can be concluded with certainty that in a diffusive model for q_e any hole boring under the above conditions stops at a density ρ not higher than 5 gcm^{-3}. The reason is that, due to pellet heating, the pressure p_0 balances the light pressure p_L. From other computer runs (Hain & Mulser, 2001) with 3-mg DT pellets, successfully ignited by $I = 2 \times 10^{20}$ W cm^{-2}, 12–16 kJ "free ignition energy," deposited at 3–5 gcm^{-3} over 20 ps and diffusively transported to the dense core without a flux limiter (therefore the low ignition energy), it can be safely concluded that hole boring or crater formation stopped at densities $\rho < 3$ gcm^{-3}. It was a common experience of the authors that, rather than a tendency to crater formation, there was a tendency to push the laser piston back, away from the deposition region, owing to a fast increase of the counterpressure p_0.

3.2. Analytical considerations

From the ignition condition $\rho R = 0.3$, at $\rho = 400$ gcm^{-3} a radius $R = 7.5$ μm results. The energy needed for ignition is typically 15 kJ (Atzeni, 1999; Mulser & Bauer, 2003). Let us now assume that the compressed core is heated by an electron beam of energy flux density q_e through one spot hemisphere during the time $\tau = 20$ ps. The energy balance $2\pi R^2 q_e \tau = 15$ kJ leads to $q_e = 2.1 \times 10^{20}$ W cm^{-2}. Surprising enough, this value agrees with the hydrodynamic beam calculations without flux limit (Hain & Mulser, 2001; see Fig. 2 therein). The comparison with the ignition energy of 75 kJ when the heat flux limit is introduced shows that in a diffusive model, most of the FI energy is not supplied to the compressed core during the phase of high compression. The location where the flux limit plays its decisive role is the high density jump behind the laser deposition region. To transport the necessary FI energy flux $q_e = 2.1 \times 10^{20}$ W cm^{-2} to the compressed core of radius $R = 7.5$ μm with

$$q_e = \kappa_0 T_e^{5/2} |\nabla T_e| \simeq \kappa_0 T_e^{7/2}/R^{-1}, \qquad \kappa_0 = 2 \times 10^{-6}\,[\text{cgsK}] \quad (7)$$

for DT ($Z = 1$; Braginskii 1966), T_e must be as high as $T_e = 34$ keV, in good agreement with the numerical simulations.

Direct heating of the pellet core by electrons produced in the critical region requires a mean free path $\lambda_e = (2 n_{DT}\sigma)^{-1}$, where σ is a Coulomb cross section, of the order of $2R$. Because the moderately relativistic differential cross section σ_Ω is $\sigma_\Omega = \gamma^{-2}\sigma_R$ (Sakurai, 1967), where σ_R is the Rutherford cross section, the total cross section σ for momentum transfer is

$$\sigma = \frac{Z^2 e^4}{4\pi\epsilon_0^2 m_e v^4 \gamma^2} \ln\Lambda, \quad \Lambda = \frac{\lambda_D}{\lambda_B}, \quad (8)$$

where λ_D is the Debye length, λ_B is the reduced de Broglie wavelength, and

$$v = \beta c, \quad \beta = \frac{u}{(1+u^2)^{1/2}}, \quad u = \frac{kT_e}{m_e c^2}, \qquad \lambda_B = \frac{\hbar}{\gamma m_e v}. \quad (9)$$

For the ratios $u = 1.0$, 1.5, and 2.0, $m_e c^2 = 511$ keV, the Coulomb logarithms for $\rho_{DT} = 400$ gcm^{-3} (corresponding to $n_{DT} = 10^{26}$ cm^{-3}) and $T_e = 40$ keV are $\ln\Lambda = 5.6$, 5.2, and 4.9, and the mean free paths λ_e amount to

$$\lambda_e(1.0) = 5.5\ \mu\text{m}, \quad \lambda_e(1.5) = 18.4\ \mu\text{m}, \quad \lambda_e(2.0) = 40.2\ \mu\text{m}.$$

https://doi.org/10.1017/S0263034604222108 Published online by Cambridge University Press

Hence, it can be concluded that electrons of $kT_e > 1.5\ m_e c_2 = 770$ keV are not stopped by an ICF pellet of standard dimensions (here: 5 mg mass and $\rho_{\max} = 400\ \mathrm{gcm}^{-3}$) and direct FI with fast electrons produced by a laser of $\lambda \gtrsim \lambda_{\mathrm{Ti:Sa}}$ fails (see Table 1) if binary collisions with cold electrons and ions are the only interaction mechanism. At $\lambda = \lambda_{\mathrm{KrF}}$ there seems to exist a possibility for FI on the basis of binary transport mechanisms as considered until now. However, one must be aware of the fact that the estimates for kT_e in Table 1 are minimum values. In addition, numerical FI studies with collimated electron beams show that the required beam energies are closer to 100 than to 10 kJ (Hain, 1999).

Owing to the lack of knowledge on energy transfer from the critical region to the target interior, hole boring can be analyzed only on the basis of more or less reasonable assumptions which, at the same time, are basic enough to allow us to come to valid conclusions.

3.2.1. Flux-limited Spitzer model

It is assumed that the energy transport from the absorption region occurs diffusively. Owing to the low collisionality q_e is nonlocal and strongly inhibited. The evolution of $p_0 = n_0 kT_{e0}$ is evaluated for $q_e = I(1-R) = 10^{21}\ \mathrm{W\,cm}^{-2} =$ const over $\tau = 20$ ps at $\lambda = 248$ nm (KrF). In a plasma of constant density, the heat diffusion equation

$$\frac{\partial T_e}{\partial t} = \frac{\kappa_0}{c_{\mathrm{V}}} \frac{\partial}{\partial x} T_e^{5/2} \frac{\partial T_e}{x}; \quad c_{\mathrm{V}} = \frac{3}{2} nk, \tag{10}$$

can be integrated for $q_e = \kappa_0 T_{\max}^{5/2} \partial T\max/\partial x =$ const under the approximation $\langle T_e \rangle = T_{\max}$. By observing that $q_e = c_{\mathrm{V}} \langle T_e \rangle x_{\mathrm{F}}$, a straightforward calculation leads to the evolution of the heat front position $x_{\mathrm{F}}(t)$ as follows:

$$x_{\mathrm{F}}(t) = \left(\frac{9}{28}\right)^{2/9} \frac{\kappa_0^{2/9}}{c_{\mathrm{V}}^{7/9}} q_e^{5/9} t^{7/9}. \tag{11}$$

Interestingly enough, if $\partial T_e/\partial x$ is approximated by $T_e/x_{\mathrm{F}}(t)$, an expression for $x_{\mathrm{F}}(t)$ is obtained in which only the numerical factor $(9/28)^{2/9} = 0.78$ is replaced by 1.0 (Zel'dovich & Raizer, 1967). Owing to the strong temperature dependence of q_e, the rectangular temperature profile $T(x,t)$ is approximately preserved (or, at least, remains self-similar) when the plasma is inhomogeneous. By setting, for convenience, $n_0(x) = \hat{n} \exp(\kappa x)$, with $\kappa = \ln(h/\hat{n} m_{\mathrm{DT}})/L$ (h, L from (5)), $\hat{n} = \gamma_{\mathrm{eff}} n_c$, and integrating $x_{\mathrm{F}} = 7x_{\mathrm{F}}/9t$, $x_{\mathrm{F}}(t)$ is deduced for variable specific heat:

$$x_{\mathrm{F}}(t) = \frac{9}{7\kappa} \ln\left\{1 + \frac{7\kappa}{9}\left(\frac{9}{28}\right)^{2/9} \kappa_0^{2/9} \frac{q_e^{5/9}}{(3k\hat{n}/2)^{7/9}} t^{7/9}\right\}$$

$$\langle T_e \rangle = \frac{\kappa q_e t}{(3k/2)\hat{n}(\exp(\kappa x_{\mathrm{F}}) - 1)}. \tag{12}$$

Its derivative $\dot{x}_{\mathrm{F}}$ is consistent with $\dot{x}_{\mathrm{F}} = 7x_{\mathrm{F}}/9t$ if the second term in the bracket is much larger than 1. This is generally fulfilled except for irrelevant, very short times ($t < 2 \times 10^{-13}$ s in the following). $x_{\mathrm{F}}(t)$, $\langle T_e \rangle(t)$, and $p_0(t)$ are evaluated now for $q_e = 10^{21}$ W cm^{-2} at KrF wavelength. From Table 1 and Eq. (8), the ratio $\kappa\lambda_e = \lambda_e/L_c \simeq 10^3$ is found (λ_e is the electron mean free path, $L_c = 1/\kappa$ is the scale length at critical density, $\kappa = 640\ \mathrm{cm}^{-1}$) for which, according to Tahraoui and Bendib (2002) a heat flux inhibition factor $f_q = 1.2 \times 10^{-4}$ results, that is, in (12) $\kappa_0 = 2 \times 10^{-6}$ [cgsK] has to be replaced by $\kappa_0 = 2 \times 10^{-6} f_q = 2.4 \times 10^{-10}$. With these parameters, Table 2 is obtained. In the neighborhood of the critical density the shock wave propagates at a speed $v_0 \simeq c/20$ if $f = 0.5$ is set. Thus, the heat wave preheats the undisturbed pellet density creating in this way the counterpressure p_0. From Table 2 it follows that hole boring stops at a time below 0.5 ps at the negligible depth of approximately 4–5 μm.

The hole boring pressure here is $P_{\mathrm{A}} \simeq p_{\mathrm{L}} = (1+R)I/c = 1$ Tbar. P_{A} scales like I, p_0 roughly like $\alpha q_e/x_{\mathrm{F}} \sim I^{1/2} I^{4/9} < I$. Owing to the monotonic decrease of f_q with decreasing laser flux density, $p_0 \sim I^{\delta}$, with $\delta < \frac{1}{2} + \frac{4}{9} < 1$, hole boring reduces with decreasing intensity of irradiation. Hence, in agreement with the numerical simulation for $I \lesssim 10^{21}$ W cm^{-2}, hole boring is suppressed when flux-limited Spitzer–Braginskii-type energy transport takes place. It should be noted that f_q used here (and all similar f_q from the published literature) is strictly valid for electron distribution functions close to equilibrium, a condition which may not be fulfilled at superhigh laser intensities.

3.2.2. Anomalous electron beam stopping

At laser wavelengths of the order of 1 μm (Nd, Ti:Sa, iodine) and beam energies in the multikilojoule range the bulk of the electrons acquires energies too high to be slowed down by a standard-size ICF pellet. The situation may change only if strongly enhanced collective stopping occurs somewhere in the pellet. Fortunately there are indications of such an anomalously intensified energy exchange, from numerical simulations (Ruhl, 2002; Sentoku *et al.*, 2002), as well as from analytical and semianalytical modeling (Das & Kaw, 2001; Jain *et al.*, 2003). Anomalous effects are expected to be bounded to the neighborhood of the critical region and to decay in the more remote dense zones of the pellet owing to collisional damping and the absence of forces driving instabilities to a high saturation level.

Table 2. *Thermal wave front x_{F}, electron temperature $\langle T_e \rangle$, and electron pressure p_0 near x_{F} for absorbed laser flux $q_e = 10^{21}$ W cm^{-2} (KrF)*

t [s]	x_{F} [μm]	$\langle T_e \rangle$ [MeV]	p_0 [Tbar]
1×10^{-13}	14.7	1.2	0.7
5×10^{-13}	31.3	1.5	2.4
1×10^{-12}	40.3	1.6	4.6
1×10^{-11}	73.8	1.7	
2×10^{-11}	84.3	1.7	
7×10^{-11}	104.0	1.9	

https://doi.org/10.1017/S0263034604222108 Published online by Cambridge University Press

The alternative model in this section assumes that the more or less collimated electron jets from Table 1 are subject to collective stopping over a length of perhaps a few tens of microns. According to Das and Kaw (2001) and Jain *et al.* (2003) a quasilinear friction term $\nu_{\rm eff}$ of the order of

$$\frac{\nu_{\rm eff}}{\omega_c} \simeq 10^{-2}, \quad \omega_c = \frac{eB}{m_e}, \tag{13}$$

acts on the fast electrons. At intensities $I \simeq 10^{21}$ W cm^{-2} a self-generated magnetic field of 1 GGauss, corresponding to an electron cyclotron frequency $\omega_c = 2 \times 10^{16}$ s^{-1}, may be assumed. Hence $\nu_{\rm eff} \gtrsim 10^{14}$ s^{-1} will result and a relativistic electron moving at speed c thermalizes over a few $\lambda_e \simeq 3$ μm, typically $3\lambda_e = 10$ μm. On the basis of present understanding this means that Eqs. (12) are applicable with a flux inhibition factor $f_q \simeq 10^{-4}$, after thermalization has been achieved, to fluxes $q_e = 10^{21}$ at Ti:Sa laser wavelength too. Owing to the short thermalization time $\tau < 10^{-13}$ s^{-1} Table 2 does not change for KrF. For Ti:Sa beams, slightly higher values for $x_{\rm F}$, $\langle T_e \rangle$, and p_0 are calculated, for example, $x_{\rm F} = 43.6$ μm, $\langle T_e \rangle = 1.7$ MeV, $p_0 = 2.7$ Tbar at $t = 5 \times 10^{-13}$ s^{-1}.

4. CONCLUSION

The foregoing analysis on fast ignition of a fusion pellet with super-intense laser beams has revealed two important aspects:

1. The energy requirements are such that the average kinetic energy of the electrons, created at laser wavelengths $\lambda \simeq 1$ μm (Nd, Ti:Sa, iodine), is too high to allow stopping in the pre-compressed pellet by binary collisions. In this situation of weak electron–pellet interaction, moderate hole boring, induced mainly by light pressure, takes place but pellet ignition fails. At laser beam wavelengths $\lambda \lesssim \lambda_{\rm Nd}/4$ (KrF) pellet ignition cannot be categorically excluded on the basis of collisional interaction only. However, then very quickly a thermal pressure exceeding the light pressure is generated and hole boring is stopped. Numerical studies confirm the analytical findings.
2. Fast ignition with acceptable laser energies in the infrared (and perhaps in the near UV too) requires anomalous, that is, collective, electron beam–pellet interaction somewhere in the moderately compressed pellet region, with the consequence that hole boring is suppressed again.

Hence, on the basis of present knowledge on electron beam–plasma coupling, we conclude that with fast ignition with energies not exceeding 100 kJ considerably, fast ignition and hole boring exclude each other.

ACKNOWLEDGMENT

Discussion of some special gas dynamic aspects with M. Kanapathipillai is gratefully acknowledged.

REFERENCES

Atzeni, S. (1999). Inertial fusion fast ignitor: Igniting pulse parameter window vs the penetration depth of the heating particles and the density of the precompressed fuel. *Phys. Plasmas* **6**, 3316–3326.

Braginskii, S.I. (1966). Transport processes in plasmas. In *Review of Plasma Physics* (Leontovich, M.A., Ed.) Vol. 1 New York: Consultants Bureau, p. 209.

Das, A. & Kaw, P. (2001). Non-local sausage-like instability of current channels in electron magnetohydrodynamics. *Phys. Plasmas* **8**, 4518–4523.

Feurer, T., Theobald, W., Sauerbrey, R., Uschmann, I., Altenbernd, D., Teubner, U., Gibbon, P., Forster, E., Malka, G. & Miquel, J.L. (1997). Onset of diffuse reflectivity and fast electron flux inhibition in 528-nm-laser solid interactions at ultrahigh intensity. *Phys. Rev. E* **56**, 4608–4614.

Hain, S. (1999). *Propagation of Intense Laser Radiation through Matter*. Herdecke, Germany: GCA-Verlag (in German); p. 128.

Hain, S. & Mulser, P. (2001). Fast ignition without hole boring. *Phys. Rev. Lett.* **86**, 1015–1018.

Jain, N., Das, A., Kaw, P. & Sengupta, S. (2003). Nonlinear electron magnetohydrodynamic simulations of sausage-like instability in magnetic channels. *Phys. Plasmas* **10**, 29–36.

Kodama, R., Norreys, P.A., Mima, K., Dangor, A.E., Evans, R.G., Fujita, H., Kitagawa, Y., Krushelnick, K., Miyakoshi, T., Miyanaga, N., Norimatsu, T., Rose, S.J., Shozaki, T., Shigemori, K., Sunahara, A., Tampo, M., Tanaka, K.A., Toyama, Y., Yamanaka, Y. & Zepf, M. (2001). Fast heating of ultrahigh-density plasma as a step towards laser fusion ignition. *Nature* **412**, 798–802.

Lindl, J. (1995). Development of the indirect-drive approach to inertial confinement fusion and the target physics basis for ignition and gain. *Phys. Plasmas* **2**, 3933–4024.

Mulser, P. & Bauer, D. (2004). Fast ignition of fusion pellets with superintense lasers: Concepts, problems, and prospectives. *Laser and Part. Beams* **22**, 5–12.

Ruhl, H. (2002). 3D kinetic simulation of super-intense laser-induced anomalous transport. *Plasma Sources Sci. Technol.* **11**, A1 A5.

Ruhl, H., Macchi, A., Mulser, P., Cornolti, F. & Hain, S. (1999). Collective dynamics and enhancement of absorption in deformed targets. *Phys. Rev. Lett.* **82**, 2095–2098.

Sakurai, J.J. (1967). *Advanced Quantum Mechanics*. Reading, MA: Addison-Wesley Publishing Co. p. 193.

Sentoku, Y., Mima, K., Sheng, Z.M., Kaw, P., Nishihara, K & Nishikawa, K. (2002). Three-dimensional particle-in-cell simulations of energetic electron generation and transport with relativistic laser pulses in overdense plasmas. *Phys. Rev. E* **65**, 046408.

Tahraoui, A. & Bendib, A. (2002). Collisional heat flux in laser heated plasmas. *Phys. Plasmas* **9**, 3089–3097.

Zel'dovich, Ya.B. & Raizer, Yu.P. (1967). *Physics of Shock Waves and High-Temperature Hydrodynamic Phenomena*. New York: Academic Press, Chap. X.